Journal of Sound and Vibration (2000) **232**(2), 431–447
doi:10.1006/jsvi.1999.2749, available online at http://www.idealibrary.com on IDEAL®

THE SOUND RADIATION EFFICIENCY OF FINITE LENGTH ACOUSTICALLY THICK CIRCULAR CYLINDRICAL SHELLS UNDER MECHANICAL EXCITATION I: THEORETICAL ANALYSIS

C. WANG AND J. C. S LAI

Acoustics and Vibration Unit, University College, The University of New South Wales, Australian Defence Force Academy, Canberra, ACT 2600, *Australia*

(*Received* 14 *January* 1999, *and in final form* 12 *October* 1999)

The acoustic radiation from circular cylindrical shells is of fundamental and applied interest primarily because cylindrical shells are widely used in industry, and because their acoustic behaviour is different from that of beams and plates due to curvature effects. In previous studies of the subject, cylindrical shells have been categorized into acoustically thin and acoustically thick shells in terms of the ratio between the ring frequency f_r and the critical frequency f_C, i.e., $f_r/f_C < 1$ for acoustically thin shells, and $f_r/f_C > 1$ for acoustically thick shells. For acoustically thin shells, it has been found by statistical methods that the radiation efficiency has a peak at the ring frequency. Above the ring frequency, the shells behave like flat plates. For acoustically thick shells, especially with finite length, however, the behavior is not so clear. From the analysis in the wavenumber domain, a formula for calculating the modal radiation efficiency of finite length circular cylindrical shells (immersed in light fluid) under mechanical excitation is obtained analytically. Based on this method, the modal-averaged sound radiation efficiencies of acoustically thick circular cylindrical shells are calculated. It is found that unlike acoustically thin shells, the radiation efficiencies of acoustically thick cylindrical shells very much depend on the acoustic behaviour of each individual vibration mode, and thus on the geometries and the boundary conditions. Results obtained by acoustic boundary element calculations and experiments verify these conclusions.

1. INTRODUCTION

Plane, spherical and cylindrical sources are generally treated as basic sound sources because of their simple geometries and their many practical applications. However, the cylindrical source has usually been treated by assuming infinite length because the corresponding solution could be expressed analytically by a series of cylindrical waves [1]. Obviously, in practice, because most circular cylindrical structures are finite in length, and the end effects become more important as the length becomes shorter, the results obtained by using an infinite length model could be in severe error. Acoustically thick shells (of which the critical frequency is lower than the ring frequency) are very common in industries; for instance, pipes of relatively small diameters and the casing of some electric machines such as motors/generators.

The acoustic properties of finite length cylindrical shells have been studied over the years, and various aspects of the acoustic radiation properties have been published. According to Fyfe and Ismail [2], the techniques used in the literature could be categorized into two groups, namely statistical approach and deterministic analysis.

0022-460X/00/170431 + 17 $35.00/0

Statistical approach [3, 4] is employed when the resonant frequencies are densely packed in the frequency band, and the acoustic properties are lumped together so that individual frequency analysis becomes impractical. Obviously, this method is only valid at high frequencies. The most successful work on a cylindrical source was carried out by Szechenyi [4], who developed a set of general, but approximate equations for predicting the radiation efficiencies of cylindrical shells having large length to thickness and radius to thickness ratios within a given frequency bandwidth. These results have been verified by experiments except for low frequencies [4].

In deterministic analysis, individual vibration velocity distributions which could be affected by the geometry and the boundary conditions of a cylindrical shell at each frequency are considered. Various studies using deterministic analysis have been reported. For example, Bordoni and Gross [5] calculated the sound power radiated from a rigid cylinder with one oscillating end surface; Williams [6] employed an approximate series method to analyze the radiation of finite length cylinders with a uniform radial vibration velocity profile; Daw and Perreira [7] studied the axial oscillations of finite length cylinders; Richards [8] concentrated on the radiation efficiency of infinite beam-like cylinders in flexural vibration; Stepanishen [9] and Zhu [10] discussed the radiation impedance and "relative sound intensities" of different vibration modes of an infinite cylinder with finite length vibration distribution respectively. Furthermore, by taking into account the reaction of the fluid inside a cylindrical shell, Stepanishen [11] studied the coupling between the acoustic modes and the structural vibration modes; Holmer and Heymann [12] investigated the sound transmission through pipe walls; and Laulagnet and Guyader [13] analyzed the acoustic radiation of a cylindrical shell immersed in light and heavy fluids. Nevertheless, the acoustic radiation of finite length acoustically thick circular cylindrical shells under mechanical excitation is not clearly understood, even when the ambient medium is light.

Due to the wide application of these shell structures, very often, the acoustic radiation from such structural elements is of great interest. However, since the modal densities of acoustically thick shells are normally low, and the corresponding ring frequencies are high, Szechenyi's statistical results are not applicable. Actually at low frequencies, because the individual behavior of each mode is becoming important, the corresponding modal-averaged radiation efficiency could have different characteristics from that at high frequencies. Therefore, a deterministic analysis of such problems would be beneficial.

The objective of this study was to conduct a detailed acoustical analysis of the sound power produced by finite length acoustically thick circular cylindrical shells under mechanical excitation, for which the modal densities are not high enough to apply statistical analysis. A formula for calculating the modal radiation efficiencies of the cylindrical shell loaded with light fluid is derived. The effects of the geometries and the boundary conditions on the modal-averaged radiation efficiency are discussed. These analytical results are compared with those obtained by acoustic boundary element calculations and experiments.

2. A REVIEW OF PREVIOUS WORK

In order to decide how to carry out the analysis, it is necessary to summarize the previous relevant work on cylindrical shells [4, 12–14] in detail.

2.1. PREVIOUS WORK

As pointed out by Wang and Lai [15], the ring frequency (f_r) is an important parameter used to indicate the frequency range for which curvature effects are important. The ring

frequency is defined as the frequency when the wavelength of extensional waves in the shell is equal to the shell circumference:

$$f_r = \frac{1}{2\pi a}\sqrt{\frac{E}{\rho}}, \tag{1}$$

where a is the radius of the cylindrical shell, ρ is the density of the material, and E is Young's modulus. For acoustic purpose, normally another important frequency should be defined, namely the critical frequency f_c. The critical frequency is the frequency at which the acoustic wavelength in the medium is the same as that in the structure. For flat plates, of which the effects of the critical frequency have been discussed thoroughly [14], this frequency has been shown to be an inherent property of the structure:

$$f_c = \frac{c_0^2}{2\pi h}\sqrt{\frac{12\rho(1-\mu^2)}{E}}, \tag{2}$$

where c_0 is the sound speed in the fluid medium such as air, h is the thickness of the plate, and μ is the Poisson ratio. Based on these two frequencies, cylindrical shells can be classified into acoustically thin shells for $f_r/f_c < 1$, and acoustically thick shells for $f_r/f_c > 1$ [12]. It should be emphasized that a shell can be geometrically thin (thickness $h \ll$ radius a) but still acoustically thick. For example, for an aluminium (Young's modulus, $E = 7{\cdot}1 \times 10^{10}\,\mathrm{N/m^2}$, density, $\rho = 2700\,\mathrm{kg/m^3}$ and the Poisson ratio, $\mu = 0{\cdot}33$) or steel ($E = 2{\cdot}60 \times 10^{10}\,\mathrm{N/m^2}$, $\rho = 7850\,\mathrm{kg/m^3}$ and $\mu = 0{\cdot}3$) circular cylindrical shell, by using equations (1) and (2), we obtain $f_r/f_c \simeq 67\,h/a$. If a/h is smaller than 67, the shell would be considered to be acoustically thick but still geometrically thin.

For acoustically thin cylindrical shells, because of the high modal density, statistical analysis can be employed [3, 4]. According to Szechenyi [4], when $f_c > f_r$, the radiation efficiency of cylindrical shells has three distinguished features corresponding to three frequency ranges. Below the ring frequency, the radiation efficiency increases at a rate of 3–6 dB per octave to a maximum at the ring frequency. Above the ring frequency, the curvature effects are no longer important and the cylindrical shells vibrate like flat plates. Therefore in the frequency range between f_r and f_c, the radiation efficiency would first decrease then increase as the frequency approaches f_c in a manner similar to flat-plate radiation. Above the critical frequency, the radiation efficiency then maintains a value of unity. In the analysis, Szechenyi also found that below the ring frequency, the modal-averaged radiation efficiency is a function of h/a, irrespective of the length and thus the boundary conditions. Moreover, the influence of the length and the boundary conditions for acoustically thin shells is only observed in the region $f_r < f < f_c$ in the same manner as flat-plate radiation. In practice, a typical example of acoustically thin shells is an airplane fuselage.

However, most practical cylindrical shells encountered in industries are acoustically thick for which Szechenyi's results [4] cannot be applied. Currently, for acoustically thick cylindrical shells, the physical significance of f_c is not clear because curvature effects would play an important role in determining the flexural wave speed and the acoustic radiation behavior. By analyzing the sound transmission through pipe walls, it has been shown [12] that the radiation efficiency of an acoustically thick cylindrical shell under the acoustic excitation normally increases smoothly with frequency until it reaches a constant value of about unity at high frequencies, and the coupling between the acoustic modes and the structural modes has to be considered. However, as pointed out by Fahy [14], the acoustic behavior of acoustically thick shells is strongly influenced by the nature and the type of the excitation. For example, the mechanical excitation of pipes can produce quite different

radiation efficiencies from those associated with excitation by fluid flow or sound waves in the internal fluid. The acoustic radiation of a cylindrical shell subjected to a point force excitation was studied by Laulagnet and Guyader [13] theoretically. They found that for light fluid (in which the ratio of its specific impedance to the angular frequency is negligible compared to the shell mass per unit area), the coupling between the acoustic modes and the structural modes is negligible. However, their cylindrical shell was acoustically thin, and no experimental results were presented.

In our preliminary study [16], the acoustic behavior of an acoustically thick steel cylindrical shell, 200 mm long, 1·6 mm thick and 63·5 mm in radius, under mechanical point excitation has been investigated. The critical and ring frequencies of this shell are 7392 and 13 190 Hz respectively. By using an acoustic boundary element code, SYSNOISE version 5·2 [17] on a SUN SPARC workstation, the radiation efficiencies of the cylindrical shell with three different boundary conditions, namely simply supported, free and clamped at both ends, have been calculated from 300 Hz to 8 kHz with a step of 100 Hz. The number of nodes and elements of the BEM model is 2480 and 2400 respectively. As a result, the number of elements per acoustic wavelength below 8 kHz is greater than 6. The analysis option used in the calculation was BEM indirect coupled analysis [17]. The results are shown in Figure 1(a). It can be seen that depending on the boundary conditions, the radiation efficiency reaches unity at a frequency much lower than the critical frequency f_c. On the other hand, Szechenyi's results for acoustically thin shells are independent of the boundary conditions. Although Szechenyi's results display a general trend similar to the BEM results, there are significant quantitative differences. Another two steel cylindrical shells, each 3 mm thick, and 19·5 mm in radius, but 20 and 60 mm in length respectively, were also examined with free-free boundary condition under point excitation. The critical and the ring frequencies for these two shells are 4036 Hz and 41·9 kHz respectively. The number of elements for the two models is 1000 and 3000 respectively. The number of elements per acoustic wavelength below 5 kHz is greater than 6 for both models. The results obtained by using the same option in SYSNOISE are shown in Figure 1(b). It can be clearly seen that for a thick shell, different lengths result in significant differences in acoustic radiation. In contrast, Szechenyi's results which are only valid for acoustically thin shells are independent of the length (Figure 1(b)). These preliminary results thus indicate that acoustically thick shells do warrant a more detailed study.

2.2. QUALITATIVE ANALYSIS

Since the radiation properties of acoustically thick cylindrical shells are strongly influenced by the geometries and the boundary conditions, statistical analysis cannot be used. Thus, the effects of each vibration mode on the acoustic radiation have to be studied. The model used here is a steel circular cylindrical shell, 200 mm long, 1·6 mm thick and 63·5 mm in radius.

It has been shown by Wang and Lai [15] that the relationships between natural frequencies and wavenumbers of finite length cylindrical shells are independent of the boundary conditions. In order to simplify the discussions, an approximate solution to the exact relationship as a result of neglecting in-plane defection [18] is used here:

$$\omega_{mn}^2 = \frac{D}{\rho h}[k_{zm}^2 + k_{\theta n}^2]^2 + \frac{K(1-\mu^2)}{\rho h a^2} \cdot \frac{k_{zm}^4}{[k_{zm}^2 + k_{\theta n}^2]^2} \tag{3}$$

where $D = Eh^3/12(1-\mu^2)$, $K = Eh/(1-\mu^2)$, ω_{mn} is the natural frequency of a circular cylindrical shell for mode (m, n), k_{zm} and $k_{\theta n}(= n/a)$ are the structural wavenumbers in the

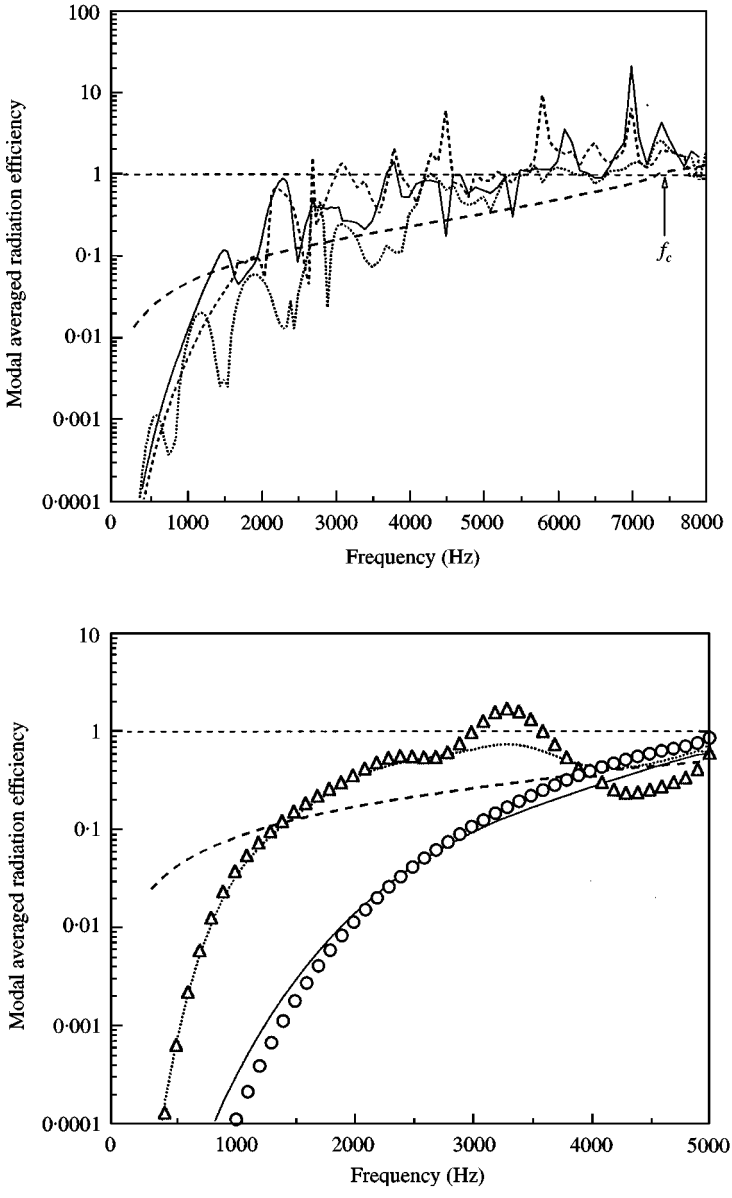

Figure 1. Modal averaged radiation efficiency of acoustically thick cylindrical shells calculated by BEM. (a) $a = 63{\cdot}5$ mm, $h = 1{\cdot}6$ mm, $l = 200$ mm; —— simply supported; ····· free–free; - - - - - clamped–clamped; - - - - Szechenyi's result. (b) $a = 19{\cdot}5$ mm, $h = 3$ mm; ○ equation (22), $l = 20$ mm; △ equation (22), $l = 60$ mm; —— BEM results, $l = 20$ mm; ····· BEM results, $l = 60$ mm; - - - - - Szechenyi's result.

axial and circumferential directions respectively. For different boundary conditions, k_{zm} takes different forms as discussed in reference [15].

In Figure 2(a), based on equation (3), a series of structural wavenumber curves associated with different frequencies are presented. It can be seen that, unlike flat plates, the vibration modes of shells having the same natural frequencies can have different structural wave numbers k_s; for instance, the wavenumbers at 13 kHz in Figure 2(a), where $k_s^2 = k_{zm}^2 + k_{\theta n}^2$.

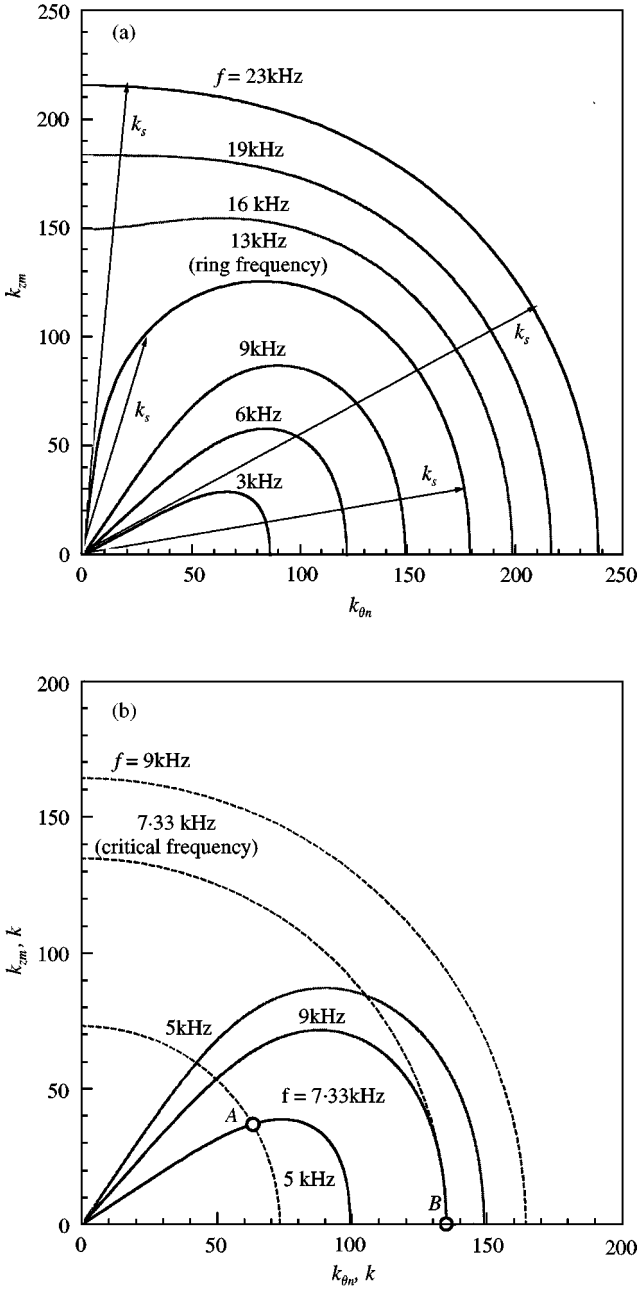

Figure 2. Wavenumber diagram for a cylindrical shell: - - - - -, acoustic wavenumber; ——, structural wavenumber; $k_{\theta n}$, circumferential structural wavenumber; k_{zm}, axial structural wavenumber; k, acoustic wavenumber.

Only above the ring frequency of the cylindrical shell would these wavenumbers approach the same value. This phenomenon is due to the curvature effects which modify the wave speed in the axial direction below the ring frequency. Thus, the effect of curvature on acoustic radiation of finite length cylindrical shells has to be examined.

In order to illustrate the curvature effects, three structural wavenumber curves and three corresponding acoustic wavenumber curves are plotted in Figure 2(b). From the acoustics point of view [14], the vibration modes could be categorized into acoustically fast modes and acoustically slow modes, sometimes called supersonic and subsonic modes. Acoustically fast modes refer to those of which the structural wavenumbers are smaller than the corresponding acoustic wavenumbers, and the modal radiation efficiencies [14] of these modes are unity. Acoustically slow modes are inefficient in acoustic radiation because structural wavenumbers are greater than the corresponding acoustic wavenumbers, which would lead to some cancellation in the radiation. For isotropic and flat plates [14, 18], the unique demarcation for these two cases is the critical frequency. However, for cylindrical shells, it can be seen from Figure 2(b) that, below the critical frequency, the structural wavenumber curve always intersects the acoustic wavenumber curve, such as point A, at a given frequency. This point of intersection in the wavenumber domain changes as the frequency changes. When the frequency is the critical frequency, the curves are tangent to each other as shown by Point B in Figure 2(b). When the frequency is greater than the critical frequency, the two curves no longer meet. This result indicates that at any frequencies below the critical frequency, acoustically fast modes and slow modes exist simultaneously, and the demarcation depends on the frequency. Therefore, for cylindrical shells, it is impossible to define a unique "critical frequency" for describing the acoustic properties as for flat plates. Figure 2(b) shows that the critical frequency defined for plates indicates the condition for all possible vibration modes of cylindrical shells to be supersonic. Thus, the radiation efficiency of cylindrical shells should be unity above the critical frequency because the modal radiation efficiencies of all modes are unity.

Below the critical frequency, since both supersonic and subsonic modes exist simultaneously, the overall radiation efficiency depends on the number and the types of modes dominating the vibration response. For example, if the mode is supersonic, the modal radiation efficiency is unity, and if it is subsonic, the modal radiation efficiency is less than one. Three points associated with the determination of the radiation efficiency below the critical frequency can be concluded here. Firstly, the demarcation for each mode, i.e., whether the mode is supersonic or not, has to be determined. Secondly, the modal-averaged radiation efficiency could be unity if supersonic modes dominate the response. Thirdly, for a given cylindrical shell, the modal-averaged radiation efficiency [14] is dependent on the excitation and boundary conditions because the excitation determines the modal amplitude and any changes of boundary conditions could make some supersonic modes subsonic or *vice versa*. By comparisons, for flat plates, all the modes occurring below the critical frequency are always subsonic and all those above the critical frequency are always supersonic [14, 18]. Therefore, it can be expected that the variation of the modal-averaged radiation efficiency of cylindrical shells due to the change of boundary conditions could be larger than that for flat plates.

In order to explain why the radiation efficiency reaches unity well below the critical frequency as shown in Figure 1(a), the model presented above will be further examined here. The natural frequencies of that cylindrical shell can be calculated according to the method described in reference [15]. Corresponding to each natural frequency, there must exist a structural wavenumber curve to which the vibration mode belongs and an acoustic wavenumber curve of the same frequency, as shown in Figure 2(b). Note that at each point of the intersection of the two curves, the structural wavenumber is equal to the acoustic wavenumber. Hence one can compare the structural wavenumber of this mode k_S with the acoustic wavenumber k to determine whether this mode is supersonic or not. For this

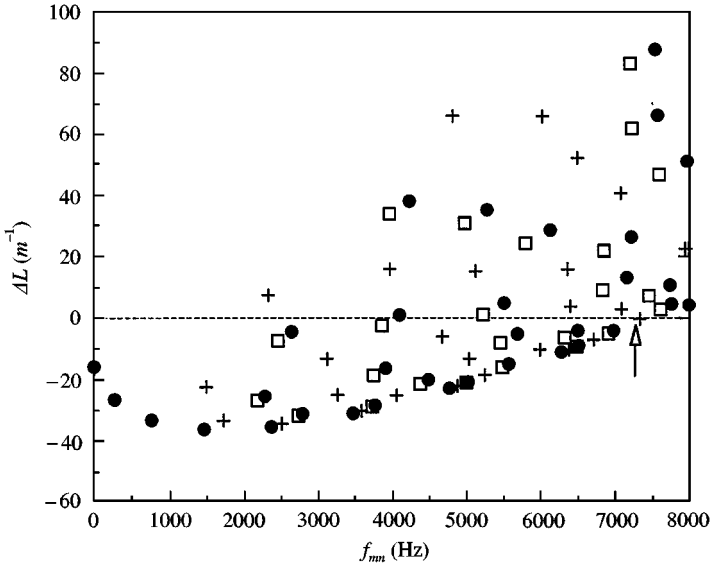

Figure 3. The index ΔL of each vibration mode of the cylindrical shell: +, simply supported; ○, free–free; □, clamped–clamped.

purpose, an index can be defined as

$$\Delta L(m,n) = k - k_s = \frac{\omega_{mn}}{c} - \sqrt{k_{zm}^2 + k_{\theta n}^2}\,. \tag{4}$$

Obviously, this index depends on the natural frequency and the structural wavenumbers of the vibration mode (m,n). If $\Delta L \geqslant 0$, which means that the acoustic wavenumber is greater than the structural wavenumber, the mode is supersonic, and if $\Delta L < 0$, the mode is subsonic. In Figure 3, ΔL of all the vibration modes associated with three different boundary conditions (simply supported, free and clamped) is plotted against their own natural frequencies. It can be seen that the critical frequency f_c of the equivalent flat plate indicates whether all the vibration modes of the cylindrical shell are supersonic or not. Below the critical frequency, corresponding to each supersonic mode in Figure 3, there is a peak in the modal-averaged radiation efficiency in Figure 1(a); for instance, the peaks around 2300 Hz for simply supported and clamped conditions, 2800 Hz for free conditions, etc. According to Figure 3, although subsonic modes exist below the critical frequency, the number of supersonic modes increases as the frequency increases so that the modal-averaged radiation efficiency could reach unity at a frequency much lower than the critical frequency, as shown in Figure 1(a).

3. THEORETICAL ANALYSIS

3.1. MODAL RADIATION EFFICIENCY

The determination of the radiation efficiency of structures analytically has always been a subject of interest to acousticians. Normally, structures with infinite dimensions, such as infinite plates and infinite length cylindrical shells [14, 18], could have simple and closed-form solutions because only approaching waves both in the structure and in the acoustic

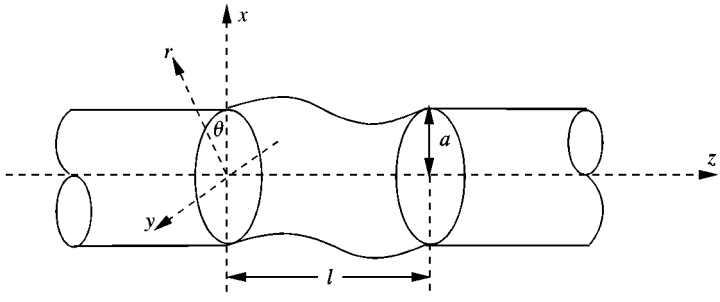

Figure 4. The finite length cylindrical shell model.

field need to be considered so that the coupling between the structure and the acoustic field can be easily handled. For structures with finite dimensions, one has to use an approximate series method to approach the exact solution [6], or alternatively to choose a theoretical model which reflects the nature of the practical structure [8–13]. For the latter approach, the accuracy strongly depends on the model selected.

In order to examine the effects of finite length, an infinite length circular cylindrical shell but with finite length vibration distribution, as shown in Figure 4, is used. This model has been employed by many researchers [9–13] in their studies using cylindrical co-ordinates. In this study, the sound field inside the cylindrical shell and the effects of internal sound field on the structural vibration and the outer sound field are not considered. For cylindrical shell structures, this might be acceptable when the shell is excited mechanically and the fluid inside the cylindrical shell is light, such as air. The surface normal displacement of each vibration mode has the form $\tilde{u}_{mnr}(\theta, z, t) = u_{mnr}\gamma_m(z)\cos(n\theta - \phi_r)e^{j\omega t}$ in the region $0 < z < l$, and zero outside this region, where u_{mnr} is the modal amplitude in the radial (r) direction for mode (m, n), and ϕ_r is a constant associated with the phase angle. Here the mode shape in the axial direction $\gamma_m(z)$ depends on the boundary conditions at $z = 0$ and l. Note that generally the vibration and corresponding acoustic solutions in the two orthogonal directions (z and θ) can be treated separately and that the vibration displacement of a circular cylindrical shell in the circumferential direction (θ) always takes the cosine form. Then by transforming $\gamma_m(z)$ to the wavenumber domain [14, 18] we have

$$\Gamma_m(k_z) = \int_0^l \gamma_m(z)e^{jk_z z}\,dz, \tag{5}$$

where $\Gamma_m(k_z)$ and $\tilde{u}_{mnr}(z, \theta, t)$ satisfy

$$\tilde{u}_{mnr}(z, \theta, t) = \frac{e^{j\omega t}u_{mnr}}{2\pi}\int_{-\infty}^{\infty}\Gamma_m(k_z)e^{-jk_z z}\,dk_z\cos(n\theta - \phi_r). \tag{6}$$

These two equations indicate that the finite vibration distribution can be decomposed into a number of waves propagating along an infinite length cylindrical shell with different wavenumbers and different amplitudes and phases. Therefore, the present problem is reduced to that of the sound radiation from an infinite length cylindrical shell with the vibration displacements of the form $u_{mnr}\Gamma_m(k_z)e^{-jk_z z}\cos(n\theta - \phi_r)$. Associated with each vibration component, the sound pressure produced in the free field is [14]

$$p_{mn}(k_z) = A\mathrm{H}_n^{(2)}(k_r r)\cos(n\theta - \phi_r)e^{-jk_z z}e^{j\omega t} \tag{7}$$

and the corresponding acoustic particle velocity is

$$V_{mn}(k_z) = -\frac{1}{\mathrm{j}\omega\rho_0}\frac{\partial P_m(k_z)}{\partial r} = \frac{\mathrm{j}A}{\omega\rho_0 k_r}\frac{\mathrm{dH}_n^{(2)}(k_r r)}{\mathrm{d}(k_r r)}\cos(n\theta - \phi_r)\mathrm{e}^{-\mathrm{j}k_z z}\mathrm{e}^{\mathrm{j}\omega t}, \tag{8}$$

where $k_r = \sqrt{k^2 - k_z^2}$, $\mathrm{H}_n^{(2)}(\cdot)$ is Hankel function of the second kind, ρ_0 is the density of air, and A is a constant. By applying the boundary condition at the interface, the sound pressure for mode (m,n) in the wavenumber domain on the surface of the cylindrical shell can be expressed as [18]

$$P_{mn}(k_z)|_{r=a} = \frac{\omega^2\rho_0 u_{mnr}}{k_r}\frac{\mathrm{H}_n^{(2)}(k_r a)}{\mathrm{dH}_n^{(2)}(k_r a)/\mathrm{d}(k_r a)}\Gamma_m(k_z)\cos(n\theta - \phi_r)\mathrm{e}^{-\mathrm{j}k_z z}. \tag{9}$$

By transforming equation (9) back to the time domain, the sound pressure produced by the vibration mode (m,n) on the vibrating surface can be obtained:

$$p_{mn}|_{r=a} = \frac{\mathrm{e}^{\mathrm{j}\omega t}}{2\pi}\int_{-\infty}^{\infty}\frac{\omega^2\rho_0 u_{mnr}}{k_r}\frac{\mathrm{H}_n^{(2)}(k_r a)}{\mathrm{dH}_n^{(2)}(k_r a)/\mathrm{d}(k_r a)}\Gamma_m(k_z)\mathrm{e}^{-\mathrm{j}k_z z}\,\mathrm{d}k_z\cos(n\theta - \phi_r). \tag{10}$$

Then the acoustic power radiated by this vibration mode is found as

$$\begin{aligned} W_{mn}(\omega) &= \frac{1}{2}\mathrm{Re}\left\{\int_0^l\int_0^{2\pi} -\mathrm{j}\omega\rho_{mn}\tilde{u}_{mnr}^* a\,\mathrm{d}\theta\,\mathrm{d}z\right\} \\ &= \frac{1}{8\pi^2}\mathrm{Re}\left\{\int_0^l\int_0^{2\pi}\left[\int_{-\infty}^{\infty}\frac{-\mathrm{j}\omega^3\rho_0 u_{mnr}}{k_r}\right.\right. \\ &\quad\left.\times\frac{\mathrm{H}_n^{(2)}(k_r a)}{\mathrm{dH}_n^{(2)}(k_r a)/\mathrm{d}(k_r a)}\Gamma_m(k_z)\mathrm{e}^{-\mathrm{j}k_z z}\,\mathrm{d}k_z\cos(n\theta - \phi_r)\right] \\ &\quad\left.\times\left[\int_{-\infty}^{\infty} u_{mnr}\Gamma_m^*(k_z')\mathrm{e}^{\mathrm{j}k_z' z}\,\mathrm{d}k_z'\cos(n\theta - \phi_r)\right]a\,\mathrm{d}\theta\,\mathrm{d}z\right\}. \end{aligned} \tag{11}$$

By taking the integration over z first, equation (11) can be further reduced to

$$\begin{aligned} W_{mn}(\omega) &= \frac{1}{4\pi}\mathrm{Re}\left[\int_{-\infty}^{\infty}\frac{-\mathrm{j}\omega^3\rho_0 u_{mnr}^2}{k_r}\frac{\mathrm{H}_n^{(2)}(k_r a)}{\mathrm{dH}_n^{(2)}(k_r a)/\mathrm{d}(k_r a)}|\Gamma_m(k_z)|^2\,\mathrm{d}k_z\right] \\ &\quad\times\left[\int_0^{2\pi}\cos^2(n\theta - \phi_r)a\,\mathrm{d}\theta\right]. \end{aligned} \tag{12}$$

Since in practice the sound power is expected to be real, by using the relationship

$$\mathrm{J}_n(x)\frac{\mathrm{d}N_n(x)}{\mathrm{d}x} - N_n(x)\frac{\mathrm{dJ}_n(x)}{\mathrm{d}x} = \frac{2}{\pi x},$$

where $\mathrm{J}_n(x)$ and $\mathrm{N}_n(x)$ are the Bessel and Neumann functions, respectively, equation (12) becomes

$$W_{mn}(\omega) = \begin{cases} \displaystyle\int_{-k}^{k}\frac{\omega^3\rho_0 u_{mnr}^2|\Gamma_m(k_z)|^2}{\pi k_r^2\,|\mathrm{dH}_n^{(2)}(k_r a)/\mathrm{d}(k_r a)|^2}\,\mathrm{d}k_z, & n = 0, \\ \displaystyle\int_{-k}^{k}\frac{\omega^3\rho_0 u_{mnr}^2|\Gamma_m(k_z)|^2}{2\pi k_r^2\,|\mathrm{dH}_n^{(2)}(k_r a)/\mathrm{d}(k_r a)|^2}\,\mathrm{d}k_z, & n \neq 0. \end{cases} \tag{13}$$

From equation (13), it can be seen that if the mode shapes in the axial direction (which depends on the boundary conditions) are known, the corresponding acoustic power radiated by each vibration mode can be predicted.

From the assumed vibration displacement for the vibrating surface, the averaged mean-square velocity for mode (m, n) can be determined from

$$\langle \overline{\tilde{v}_{mnr}^2} \rangle = \frac{\omega^2}{2S} \int_0^l \int_0^{2\pi} u_{mnr}^2 \, |\gamma_m(z)|^2 \cos^2(n\theta - \phi_r) a \, \mathrm{d}\theta \, \mathrm{d}z$$

$$= \begin{cases} \dfrac{\pi\omega^2 u_{mnr}^2}{S} \displaystyle\int_0^l |\gamma_m(z)|^2 a \, \mathrm{d}z, & n = 0, \\ \dfrac{\pi\omega^2 u_{mnr}^2}{2S} \displaystyle\int_0^l |\gamma_m(z)|^2 a \, \mathrm{d}z, & n \neq 0, \end{cases} \tag{14}$$

where S is the surface area of the finite length cylindrical shell. By using the definition of modal radiation efficiency [14], the modal radiation efficiency of finite length cylindrical shells can be found as

$$\sigma_{mn}(\omega) = \frac{W_{mn}(\omega)}{\rho_0 c_0 S \langle \overline{\tilde{v}_{mnr}^2} \rangle} = \frac{k}{\pi^2} \frac{1}{\displaystyle\int_0^l |\gamma_m(z)|^2 a \, \mathrm{d}z} \int_{-k}^{k} \frac{|\Gamma_m(k_z)|^2}{k_r^2 \, |\mathrm{d}H_n^{(2)}(k_r a)/\mathrm{d}(k_r a)|^2} \, \mathrm{d}k_z . \tag{15}$$

Hence, in order to calculate the modal radiation efficiency according to equation (15), the mode shapes in the axial direction have to be determined. Note that in reference [15], it has been shown that the mode shapes of cylindrical shells in the axial direction can be determined with good approximations by using the beam function. Equation (15) can be effectively employed to calculate the modal radiation efficiencies of a finite length cylindrical shell. As equation (15) involves the ratio of two integrals, it is unlikely that a simple expression like that for infinite cylindrical shells can be obtained. However, for cylindrical shells simply supported at two ends, the mode shapes in the axial direction are given exactly by [1]

$$\gamma_m(z) = \sin \frac{m\pi z}{l} \tag{16}$$

By using this equation, $\Gamma_m(k_z)$ can be found as

$$\Gamma_m(k_z) = \frac{(m\pi/l)\,[(-1)^m \mathrm{e}^{\mathrm{j}k_z z} - 1]}{k_z^2 - (m\pi/l)^2} . \tag{17}$$

By substituting equations (16) and (17) into equation (15), we have

$$\sigma_{mn}(\omega) = \int_{-k}^{k} \frac{2kl}{\pi^2 a k_r^2 \, |\mathrm{d}H_n^{(2)}(k_r a)/\mathrm{d}(k_r a)|^2} \left[\frac{m\pi/l}{k_z + m\pi/l} \right]^2 \frac{\sin^2[l/2(k_z - m\pi/l)]}{[l/2\,(k_z - m\pi/l)]^2} \, \mathrm{d}k_z . \tag{18}$$

Generally, equations (15) and (18) have to be solved numerically to provide information on the basic properties of the modal radiation efficiency of finite length cylindrical shells.

3.2. MODAL AVERAGED RADIATION EFFICIENCY

Although the modal radiation efficiency of finite length cylindrical shells has been obtained above, it should be noted that in practice, it is the modal-averaged radiation efficiency rather than modal radiation efficiency that can be directly measured. Generally, to obtain the modal-averaged radiation efficiency, one has to work out the vibration distribution on the structure. According to Soedel [20], if the distributed loads on the cylindrical shell in the three directions are assumed as $F_z e^{j\omega t}$, $F_\theta e^{j\omega t}$, $F_r e^{j\omega t}$ (N/m^2), the steady state harmonic vibration response of mode (m, n) in the radial direction is given by

$$u_{mnri}(z,\theta) = \frac{|F_{mni}|}{\sqrt{(\omega_{mni}^2 - \omega^2)^2 - 4\zeta_{mni}^2 \omega_{mni}^2 \omega^2}}, \tag{19}$$

where

$$F_{mni} = \frac{1}{\rho h N_{mni}} \int_0^l \int_0^{2\pi} (F_z U_{mnzi} + F_\theta U_{mn\theta i} + F_r U_{mnri}) a \, \mathrm{d}\theta \, \mathrm{d}z,$$

$$N_{mni} = \int_0^l \int_0^{2\pi} (U_{mnzi}^2 + U_{mn\theta i}^2 + U_{mnri}^2) a \, \mathrm{d}\theta \, \mathrm{d}z.$$

For every m, n combination, there are three natural frequencies ω_{mni} $(i = 1, 2, 3)$ corresponding to the three vibration modes (longitudinal, torsional, and flexural); ζ_{mni} is the corresponding modal damping of the three vibration modes, and U_{mnzi}, $U_{mn\theta i}$, U_{mnri} are the mode components of the longitudinal, torsional, and flexural vibrations of the cylindrical shell respectively (see reference [20] for details). Normally, these mode shapes have the forms

$$\begin{aligned} U_{mnzi} &= \frac{A_{mni}}{C_{mni}} \alpha_m(z) \cos n(\theta - \varphi), \\ U_{mn\theta i} &= \frac{B_{mni}}{C_{mni}} \beta_m(z) \sin n(\theta - \varphi), \\ U_{mnri} &= \gamma_m(z) \cos n(\theta - \varphi), \end{aligned} \tag{20}$$

where $\alpha_m(z)$, $\beta_m(z)$, and $\gamma_m(z)$ are the mode shapes of the three vibrations along the axial direction (z) of the cylindrical shell, A_{mni}/C_{mni}, and B_{mni}/C_{mni} are the coupling ratios between the longitudinal and flexural vibrations, and between the torsional and flexural vibrations, respectively, as given by Soedel [20]. For simply supported ends, $\alpha_m(z)$, $\beta_m(z)$, and $\gamma_m(z)$ have exact solutions as [20]

$$\alpha_m(z) = \cos\left(\frac{m\pi}{l}\right), \quad \beta_m(z) = \sin\left(\frac{m\pi}{l}\right), \quad \gamma_m(z) = \cos\left(\frac{m\pi}{l}\right), \quad m = 1, 2, 3, \ldots . \tag{21a}$$

For other boundary conditions, $\alpha_m(z)$, $\beta_m(z)$, and $\gamma_m(z)$ can be approximately obtained from a longitudinally vibrating beam, and a transversely vibrating beam of the same corresponding boundary conditions respectively [20]. For example, the mode shapes of flexural vibration for free–free ends are [21]

$$\gamma_0(z) = 1, \qquad \gamma_1(z) = \frac{z}{l} - \frac{1}{2}, \tag{21b}$$

$$\gamma_m(z) = \cosh(k_{zm}z) + \cos(k_{zm}z) - \frac{\cosh(k_{zm}l) - \cos(k_{zm}l)}{\sinh(k_{zm}l) - \sin(k_{zm}l)}[\sinh(k_{zm}z) + \sin(k_{zm}z)],$$

$$k_{zm} \simeq \frac{m\pi}{l} - \frac{\pi}{2l}, \quad m = 2, 3, 4, \ldots$$

and those for clamped–clamped ends are

$$\gamma_m(z) = \cosh(k_{zm}z) - \cos(k_{zm}z) - \frac{\cosh(k_{zm}l) - \cos(k_{zm}l)}{\sinh(k_{zm}l) - \sin(k_{zm}l)}[\sinh(k_{zm}z) - \sin(k_{zm}z)],$$

$$k_{zm} \simeq \frac{m\pi}{l} - \frac{\pi}{2l}, \quad m = 1, 2, 3 \cdots . \tag{21c}$$

It has been shown in reference [15] that the exact relationships between the natural frequencies and the wavenumbers for the three vibrations are independent of the boundary conditions, and therefore so are the coupling ratios. For all the boundary conditions, the coupling ratios obtained from simply supported conditions (see reference [20] for details) can be directly used by substituting the appropriate natural frequencies.

If only F_r exists, although vibrations in the three directions would be excited, the flexural vibration would dominate the vibration response ($i = 3$). By using the definition of modal-averaged radiation efficiency [14], the modal-averaged efficiency of the cylindrical shell can be obtained from

$$\bar{\sigma}(\omega) = \frac{\sum_{m,n} \sigma_{mn} |\overline{\tilde{v}^2_{mnr}}|}{\sum_{m,n} |\overline{\tilde{v}^2_{mnr}}|} = \frac{\sum_m^\infty \sum_n^\infty (\sigma_{mn}(\omega)|F_{mn3}|^2 N_{mn3})/((\omega^2_{mn} - \omega^2)^2 - 4\varsigma^2_{mn}\omega^2_{mn}\omega^2)}{\sum_m^\infty \sum_n^\infty (|F_{mn3}|^2 N_{mn3})/((\omega^2_{mn} - \omega^2)^2 - 4\varsigma^2_{mn}\omega^2_{mn}\omega^2)}. \tag{22}$$

With equation (22), the modal-averaged radiation efficiencies of the steel circular cylindrical shells discussed in section 2.1 are calculated and compared with the BEM results (Figure 1) in Figures 5 and 1(b). In the BEM calculation, the modal damping was set as 0·001. It can be seen that for simply supported, and free–free conditions, the results obtained from equation (22) and BEM agree reasonably well. For the clamped–clamped condition, at low frequencies the curve obtained by equation (22) is shifted slightly to higher frequencies. This is because the natural frequencies predicted by using the beam function are higher than the numerical results [15]. Nevertheless, Figures 5 and 1(b) indicate that equation (22) can predict the modal-averaged radiation efficiency of circular cylindrical shells with reasonable accuracy.

According to equation (22), the contribution of each vibration mode to the response depends on the external excitation. In principle, therefore, different modal-averaged radiation efficiencies would be expected depending on the type of excitation (such as mechanical excitation or acoustic excitation), the distribution of the excitation forces (such as point force or surface force), and the positions of the application of the excitation. It seems, therefore, impossible to obtain a unique modal-averaged radiation efficiency for a given cylindrical shell. However, if all the vibration modes are excited in a strcuture, at each natural frequency, the vibration response is usually dominated by the vibration mode corresponding to this frequency. Thus, the modal-averaged radiation efficiency at $\omega = \omega_{mn}$ may be approximated by the value of the modal radiation efficiency of mode (m, n) at $\omega = \omega_{mn}$, as

$$\bar{\sigma}|_{\omega = \omega_{mn}} \simeq \sigma_{mn}(\omega_{mn}). \tag{23}$$

Since equation (23) is only valid at each natural frequency, it can be expected that the larger the separation between the two adjacent natural frequencies, the more information will be lost in that region. Therefore, the accuracy of equation (23) would improve if the modal density is high. By using equations (15), (21) and (23), the modal-averaged radiation efficiencies of the cylindrical shell model with three different boundary conditions are calculated at each natural frequency and plotted in Figures 5(a)–(c). It can be seen that except at low frequencies, say below 4000 Hz, where the number of vibration modes is less,

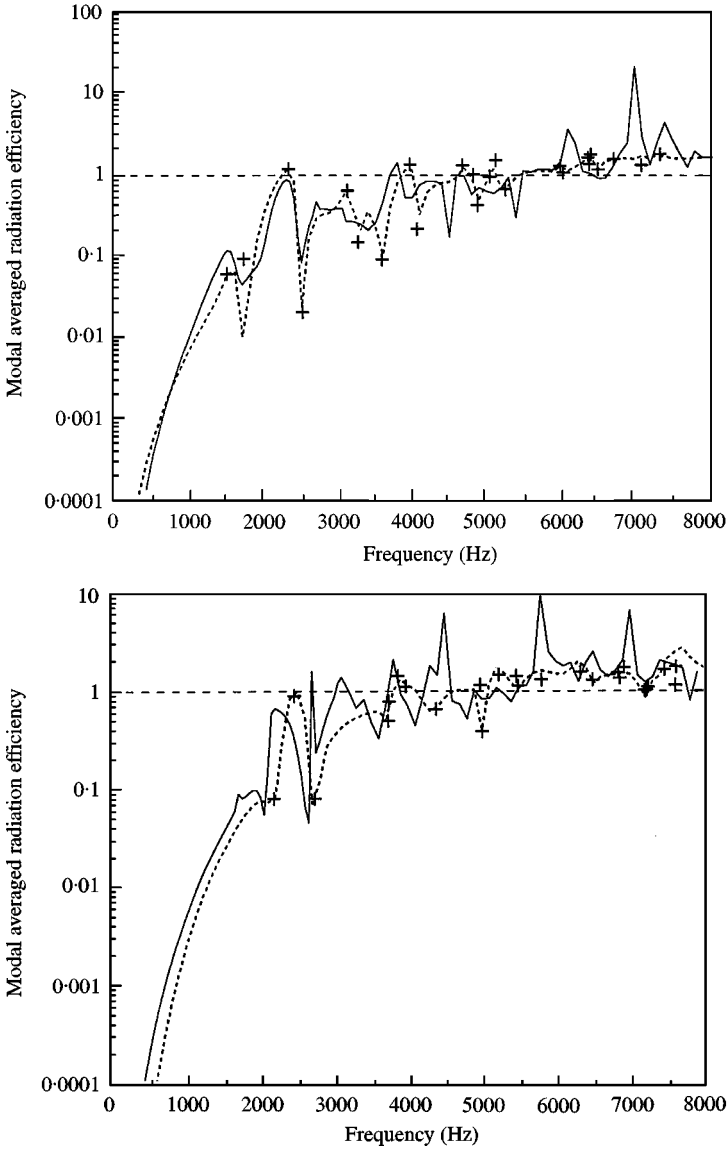

Figure 5. (a) Modal averaged radiation efficiency of a simply supported cylindrical shell: $a = 63{\cdot}5$ mm, $h = 1{\cdot}6$ mm, $l = 200$ mm; —— BEM results; ····· Equation (22); + equation (23). (b) Modal averaged radiation efficiency of a clamped–clamped cylindrical shell: $a = 63{\cdot}5$ mm, $h = 1{\cdot}6$ mm, $l = 200$ mm; —— BEM results; ..... equation (22); + equation (23). (c) Modal averaged radiation efficiency of a free–free cylindrical shell: $a = 63{\cdot}5$ mm, $h = 1{\cdot}6$ mm, $l = 200$ mm; —— BEM results; ····· equation (22); + equation (23).

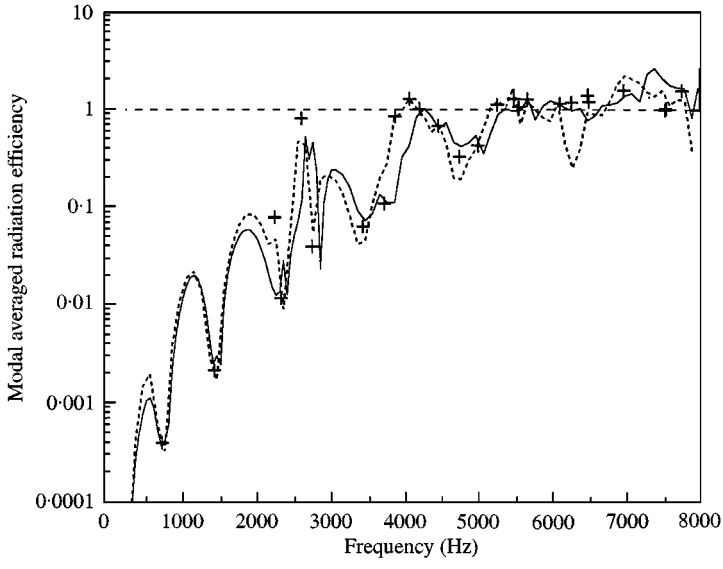

Figure 5. Continued.

the results obtained by equation (23) are good approximations. However, if the structure is excited coincidentally so that only one vibration mode exists in a wide frequency range, equation (23) may incur some errors because the assumption that each mode would dominate the response at its natural frequency is no valid here. In this case, the modal-averaged radiation efficiency ($\bar{\sigma}(\omega)$) would be equal to the modal radiation efficiency ($\sigma_{mn}(\omega)$). Therefore, the accuracy of equation (23) also depends on the number of vibration modes excited in the structure.

4. EXPERIMENT

In order to verify the above analytical and BEM results, an experiment was carried out in an anechoic room. The geometry of the cylindrical shell is the same as that in the simulation shown in Figure 1(a). Only a shell with both ends free was tested. As shown in Figure 6, the shell was excited by a B&K-type 4810 shaker driven by a B&K 2706 power amplifier. The excitation signal used was random noise from 0 to 6·4 kHz which was provided by a HP3569A dual channel analyzer. The acoustic power output from the shell was measured by scanning a sound intensity probe over the cylindrical shell. The sound intensity probe comprised two $\frac{1}{2}$ in microphones separated by 12 mm, thus giving an acceptable frequency range from 125 Hz to 5 Hz. The sound power was determined from the sound intensity spectra obtained with HP3569A and the scanned area. The vibration spectra at 70 points distributed uniformly on the shell were also measured using a B&K-type 2635 charge amplifier and a B&K-type 4383 accelerometer. All these vibration data were recorded by HP3569A and further processed to give the spatial-averaged mean-square vibration velocity over the shell. From the measured sound power and the spatial-averaged mean-square vibration velocity, the measured radiation efficiency spectrum is determined and plotted in Figure 7. It can be seen that the experimental results agree fairly well with the analytical and BEM results.

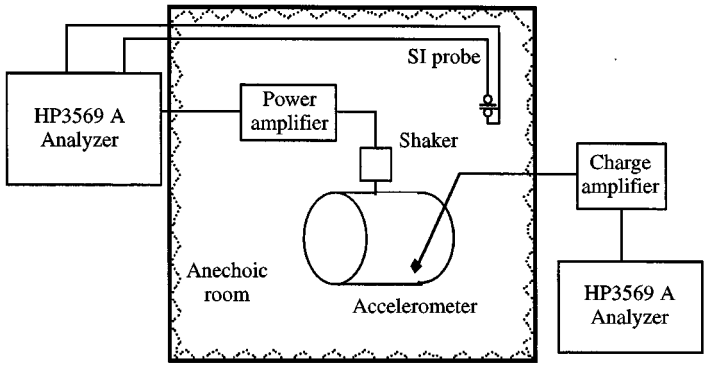

Figure 6. Schematic diagram of experimental set-up for measuring the sound radiation efficiency of a cylindrical shell: Charge amplifier, B&K 2635; power amplifier, B&K 2707; Shaker, B&K 4810; Accelerometer, B&K 4383.

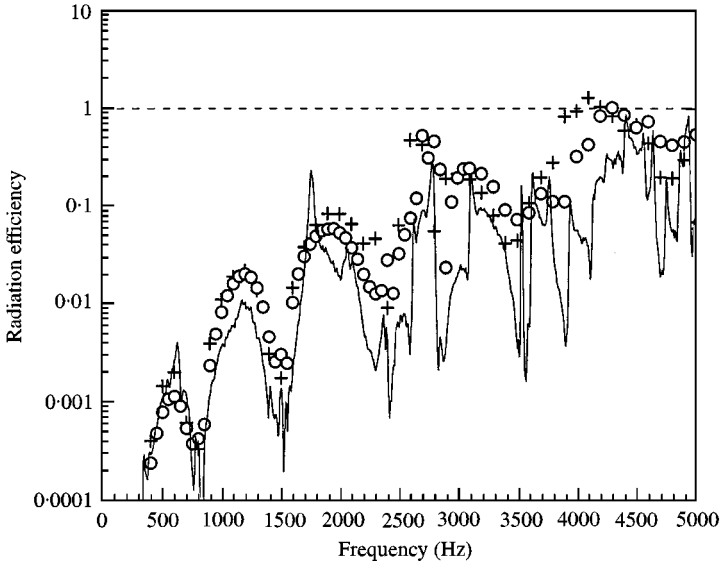

Figure 7. Comparison of the measured radiation efficiency with BEM and analytical calculations: —— measurement; ○ BEM, + equation (22).

5. CONCLUSIONS

A literature review on the acoustic radiation of finite length circular cylindrical shells has revealed that the radiation characteristics are not well understood for acoustically thick shells ($f_r/f_c > 1$) as for acoustically thin shells ($f_r/f_c < 1$). Analysis of acoustically thick shells has shown that unlike flat plates, for frequencies below the critical frequency, both supersonic and subsonic modes can exist. Consequently, the radiation efficiency is dependent on the geometries and boundary conditions and could reach unity at a frequency much lower than the critical frequency.

The modal radiation efficiency of a finite length circular cylindrical shell loaded with a light fluid has been derived using an infinite length model with vibration velocity distributed over a finite length. An approximate method introduced to calculate the

modal-averaged radiation efficiency based on the modal radiation efficiency has produced results in good agreement with boundary element calculations for simply supported, free–free and clamped–clamped boundary conditions, and with the experimental results for the free–free boundary conditions.

ACKNOWLEDGMENTS

This project was supported by the Australian Research Council under the large grant scheme. The first author (C. Wang) acknowledges receipt of an Overseas Postgraduate Scholarship for the pursuit of this study.

REFERENCES

1. P. M. MORSE 1984 *Vibration and Sound*, New York: McGraw-Hill.
2. K. R. FYFE and F. ISMAIL 1989 *Journal of Sound and Vibration* **128**, 361–375. An investigation of the acoustic properties of vibrating finite cylinders.
3. J. E. MANNING and G. MAIDANIK 1964 *Journal of the Acoustical Society of America* **36**, 1691–1698. Radiation properties of cylindrical shells.
4. E. SZECHENYI 1971 *Journal of Sound and Vibration* **19**, 65–81. Modal densities and radiation efficiencies of unstiffened cylinders using statistical methods.
5. P. G. BORDONI and W. GROSS 1949 *Journal of Mathematical Physics*, **27**, 241–252. Sound radiation from a finite cylinder.
6. W. WILLIAMS, F. G. PARKE, D.A. MORAN and C. H. SHERMAN 1964 *Journal of the Acoustical Society of America* **36**, 2316–2322. Acoustic radiation from a finite cylinder.
7. N. D. PERREIRA and D. DAWE 1984 *Journal of the Acoustical Society of America* **75**, 80–87. An analytical model for noise generated by axial oscillation of unbaffled cylindrical elements.
8. R. K. JEYAPALAN and E. J. RICHARDS 1979 *Journal of Sound and Vibration* **67**, 55–67. Radiation efficiencies of beams in flexural vibration.
9. P. R. STEPANISHEN 1978 *Journal of the Acoustical Society of America* **63**, 328–338. Radiated power and radiation loading of cylindrical surfaces with nonuniform velocity distributions.
10. Z. Q. ZHU and D. HOWE 1994 *IEE Proceedings of Electric Power Applications* **141**, 109–119. Improved methods for prediction of electromagnetic noise radiated by electrical machines.
11. P. R. STEPANISHEN 1982 *Journal of the Acoustical Society of America* **71**, 813–823. Modal coupling in the vibration of fluid-loaded cylindrical shells.
12. C. I. HOLMER and F. J. HEYMANN 1980 *Journal of Sound and Vibration* **70**, 275–301. Transmission of sound through pipe walls in the presence of flow.
13. B. LAULAGNET and J. L. GUYADER 1989 *Journal of Sound and Vibration* **131**, 397–415. Modal analysis of shell's acoustic radiation in light and heavy fluids.
14. F. FAHY 1987 *Sound and Structural Vibration—Radiation, Transmission and Response*. New York: Academic Press.
15. C. WANG and J. C. S. LAI (in press). *Applied Acoustics*. Prediction of natural frequencies of finite length circular cylindrical shells.
16. C. WANG and J. C. S. LAI 1997 *Proceedings of the 5th International Congress on Sound and Vibration, Adelaide, Australia*, Vol. **2**, 877–884. Acoustic radiation of finite length cylindrical shells with different boundary conditions using boundary element method.
17. *SYSNOISE Manual Book* 1993 Version 5.2, NIT, Belgium.
18. L. CREMER, M. HECKL and E. E. UNGAR 1988 *Structure-Borne Sound*. Berlin: Springer-Verlag.
19. L. H. DONNELL 1938 *Proceedings of the 5th International Congress of Applied Mechanics*, A discussion of thin shell theory.
20. W. SOEDEL 1993 *Vibrations of Shells and Plates*. New York: Marcel Dekker, Inc., second edition.
21. A. W. LEISSA *Vibration of Shells. NASA SP*-288.